Microbiology (2003), **149**, 1911–1921 DOI 10.1099/mic.0.26122-0

Incorporation of iron into *Tritrichomonas foetus* cell compartments reveals ferredoxin as a major iron-binding protein in hydrogenosomes

Pavel Suchan,[1] Daniel Vyoral,[2] Jiří Petrák,[2] Robert Šuťák,[1] Dominique Rasoloson,[4] Eva Nohýnková,[3] Pavel Doležal[1] and Jan Tachezy[1]

Correspondence
Jan Tachezy
tachezy@natur.cuni.cz

[1]Department of Parasitology, Faculty of Science, Charles University, Viničná 7, 128 44, Prague 2, Czech Republic

[2]Institute of Hematology and Blood Transfusion, U Nemocnice 1, 128 44, Prague 2, Czech Republic

[3]Department of the Tropical Medicine, 1st Faculty of Medicine, Charles University, Faculty Hospital Bulovka, Studničkova 7, 128 00, Prague 2, Czech Republic

[4]Johns Hopkins University, Bloomberg School of Public Health, W. Harry Feinstone Department of Molecular Microbiology and Immunology, 615 North Wolfe Street, Baltimore 21205, MD, USA

The intracellular transport of iron and its incorporation into organelles are poorly understood processes in eukaryotes and virtually unknown in parasitic protists. The transport of iron is of particular interest in trichomonads, which possess hydrogenosomes instead of mitochondria. The metabolic functions of hydrogenosomes, which contain a specific set of FeS proteins, entirely depend on iron acquisition. In this work the incorporation of iron into the cattle parasite *Tritrichomonas foetus* was monitored. Iron was efficiently taken up from ^{59}Fe-nitrilotriacetic acid and accumulated in the cytosol (88·9 %) and hydrogenosomes (4·7 % of the total radioactivity). Using atomic absorption spectrophotometry, an unusually high steady-state iron concentration in hydrogenosomes was determined [$54{\cdot}4 \pm 1{\cdot}1$ nmol Fe (mg protein)$^{-1}$]. The concentration of iron in the cytosol was $13{\cdot}4 \pm 0{\cdot}5$ nmol Fe (mg protein)$^{-1}$. Qualitative analysis of incorporated iron was performed using native gradient PAGE. The majority of the ^{59}Fe in the cytosol appeared as the labile-iron pool, which represents weakly bound iron associated with compounds of molecular mass ranging from 5000 to 30 000 Da. Ferritin was not observed in *Tt. foetus*, nor in two other anaerobic protists, *Entamoeba histolytica* and *Giardia intestinalis*. Analysis of *Tt. foetus* hydrogenosomes showed at least nine iron-binding compounds, which were absent in metronidazole-resistant mutants. The major iron-binding compound was identified as [2Fe–2S] ferredoxin of the adrenodoxin type.

Received 13 November 2002
Revised 24 February 2003
Accepted 24 March 2003

INTRODUCTION

Tritrichomonas foetus is an amitochondrial anaerobic protist, causing a sexually transmitted disease in cattle. The ability of this parasite to acquire iron from the host environment is a critical factor for its pathogenicity and virulence (Kulda *et al.*, 1998). To cover its nutritional requirements, *Tt. foetus* is able to utilize lactoferrin, transferrin or low-molecular-mass iron complexes (Tachezy *et al.*, 1996; Tachezy *et al.*, 1998). Lactoferrin is internalized via receptor-mediated endocytosis, while transferrin-bound iron and iron from low-molecular-mass complexes is acquired by means of carrier-mediated transport (Tachezy *et al.*, 1996, 1998). The high nutritional requirements of *Tt. foetus* and other amitochondrial protists such as *Giardia intestinalis* and *Entamoeba histolytica* are ascribed to the importance of FeS protein in their energy metabolism (Payne *et al.*, 1993; Ellis *et al.*, 1993; Weinbach *et al.*, 1980; Gorrell *et al.*, 1984; Müller, 1988). They possess ferredoxin-mediated low-redox potential electron transport, which is linked to pyruvate : ferredoxin oxidoreductase (PFOR), a key FeS-containing enzyme of pyruvate metabolism (Weinbach *et al.*, 1980; Brown *et al.*, 1998; Ellis *et al.*, 1993; Kulda, 1999). In trichomonads, PFOR-dependent

Abbreviations: DFO, desferrioxamine; LIP, labile-iron pool; NMML, nominal molecular mass (weight) limits; NTA, nitrilotriacetic acid; PFOR, pyruvate : ferredoxin oxidoreductase; ST, sucrose-Tris (buffer).

The GenBank accession number for the sequence reported in this paper is AF545472.

pyruvate metabolism takes place in specific ATP-generating organelles called hydrogenosomes (Dyall & Johnson, 2000; Müller, 1993). Several authors have reported that iron-restricted nutritional conditions cause a decrease in the metabolic activity of hydrogenosomes (Tachezy *et al.*, 1996; Vaňáčová *et al.*, 2001; Gorrell, 1985; Peterson & Alderete, 1984). This phenomenon are associated with a down-regulation of the genes encoding PFOR and other hydrogenosomal proteins (Vaňáčová *et al.*, 2001). Similar changes have been observed in metronidazole-resistant organisms. Metronidazole and other 5-nitroimidazoles, which are used for the treatment of trichomoniasis, are reductively activated in hydrogenosomes. The [2Fe–2S] ferredoxin is considered to be the major hydrogenosomal electron carrier responsible for drug activation. In the absence of metronidazole, ferredoxin transports electrons from PFOR to [Fe]-hydrogenase, where molecular hydrogen is formed. When metronidazole is present, the ferredoxin-transported electrons are preferentially captured by the drug, which results in a release of cytotoxic nitro-radicals (Kulda, 1999). A decreased expression or absence of ferredoxin, PFOR and other hydrogenosomal proteins has been found in metronidazole-resistant *Trichomonas vaginalis* (Rasoloson *et al.*, 2001, 2002; Quon *et al.*, 1992) and *Tt. foetus* (Land *et al.*, 2001).

The mechanisms of intracellular iron transport and its delivery to organelles are poorly understood processes in eukaryotes and virtually unknown in parasitic protists. Several authors proposed that iron is transported within the cell in a complex with low-molecular-mass ligands; however, their molecular basis remains unclear (Jacobs, 1977; Weaver & Pollack, 1989; Bohnke & Matzanke, 1995). 'Mobile' iron is also referred to as the labile-iron pool (LIP) as it is easily removed from ligands by iron chelators. It can be visualized and quantified by means of native gradient electrophoresis followed by storage phosphorimaging (Vyoral & Petrák, 1998b; Vyoral *et al.*, 1998). An alternative model for intracellular iron transport was proposed by Richardson *et al.* (1996). They suggested that iron is transported within the cell in endosomal vesicles and delivered to various cellular compartments by means of direct protein–protein contact transport without the contribution of low-molecular-mass iron ligands.

In mitochondria, iron is required for the biogenesis of FeS proteins (Lill & Kispal, 2000). The source of sulfur for FeS cluster assembly is cysteine, from which molecular sulfur is released by IscS, a PLP-dependent cysteine desulfurase (Zheng *et al.*, 1994). It is likely that in trichomonads IscS-mediated FeS cluster formation occurs within the hydrogenosomes (Tachezy *et al.*, 2001). Unlike sulfur, the source of iron is unknown in both mitochondria and hydrogenosomes. Here we use native gel electrophoresis to trace iron uptake and distribution in *Tt. foetus*. A pathway to the hydrogenosomes is defined, mediating iron accumulation in that organelle and delivery to the resident FeS protein ferredoxin.

METHODS

Organisms and culture conditions. The following strains of parasites were used in this study: *Tt. foetus* metronidazole-sensitive strain Lub-1 MIP (Tachezy *et al.*, 1996), metronidazole-resistant strain Lub-1 MR100 (Tachezy *et al.*, 1998), *G. intestinalis* strain Portland-1 (ATCC 30888) and *E. histolytica* strain HM-1 : IMSS (ATCC 30459).

Trichomonads were maintained in TYM medium (Diamond, 1957) with 10 % heat-inactivated horse serum at pH 7·2. *G. intestinalis* cells were grown in TYI-S-33 medium supplemented with 10 % heat-inactivated bovine serum and 0·1 % bovine bile at pH 6·8 (Keister, 1983). For cultivation of *E. histolytica* parasites, TYI-S-33 medium with 10 % heat-inactivated bull serum and a complex vitamin mixture was used (Diamond *et al.*, 1978). K-562 human leukaemic cells (ATCC CCL-243) were maintained in Iscove's modified Dulbecco's medium (Sigma) supplemented with 10 % fetal bovine serum.

Reagents. Bovine and human apotransferrins and lactoferrins were purchased from Sigma, desferrioxamine (DFO) was obtained from Ciba-Geigy, 1,2-dimethyl-3-hydroxypyrid-4-one (L1, Deferiprone) was kindly provided by Dr G. J. Kontoghiorges (Royal Free Hospital, London). Radiolabelled iron(III)-nitrilotriacetate (Fe-NTA) was prepared according to Bates & Wernicke (1971) using $^{59}FeCl_3$ (NEN) and NTA-disodium salt (Sigma) in a molar ratio of 1 : 4.

Iron desaturation and saturation of lactoferrin and transferrin. Bovine and human lactoferrins were iron-desaturated according to Mazurier & Spik (1980). Saturation of apolactoferrin and apotransferrin with iron using the ^{59}Fe-NTA complex was performed as described previously (Tachezy *et al.*, 1996). The proteins were about 80–95 % iron-saturated as determined by incorporated radioactivity. Non-radioactive diferric transferrin was prepared by the same method using a non-radioactive Fe-NTA complex.

Growth experiments. To test iron-dependent stimulation of cell growth, TYM and TYI-S-33 media were depleted of iron by addition of 100 μM 2,2-dipyridyl and supplemented with serial concentrations of Fe-NTA, Fe-transferrin or Fe-lactoferrin. *Tt. foetus* suspensions [1×10^5 cells (ml depleted medium)$^{-1}$] were placed on 96-well microtitre plates (250 μl aliquots per well) and the plates were incubated in anaerobic jars at 37 °C for 30 h. *G. intestinalis* and *E. histolytica* aliquots of 1 ml (1×10^5 cells) per well were placed on 24-well microtitre plates and incubated for 48 and 72 h, respectively. Cultivation was stopped by addition of 25 μl 1 % formaldehyde in PBS per well and, prior to counting, the plates were left for 3–12 h in a refrigerator which led to quantitative detachment of the formaldehyde-fixed cells.

Incorporation of [^{59}Fe]iron. The parasites were washed three times in NaCl-HEPES buffer (0·14 M NaCl, 10 mM HEPES, pH 7·4), resuspended to a density of 5×10^7 ml^{-1} and 100 μl aliquots were placed into 1·5 ml microtubes. The cells were preincubated at 37 °C for 15 min. Subsequently, NaCl-HEPES buffer and ^{59}Fe-NTA, ^{59}Fe-transferrin or ^{59}Fe-lactoferrin were added to the cell suspension to give 150 ng Fe ml^{-1} in a final volume of 250 μl. The cells were incubated at 37 °C for 60 min, washed three times in NaCl-HEPES buffer to remove the unbound radioactivity and stored at −70 °C until further processing.

Subcellular fractionation. *Tt. foetus* cells (5×10^8) were incubated with ^{59}Fe-NTA as described above in 25 ml NaCl-HEPES buffer. The parasites were washed three times in sucrose-Tris (ST) buffer (0·25 M sucrose, 10 mM Tris, 0·5 mM KCl, pH 7·2) to remove the unbound radioactivity and resuspended at a density of about 5×10^8 cells ml^{-1}. Cytosolic, microsomal, hydrogenosomal and lysosomal fractions were obtained by means of differential and gradient centrifugation. All steps were performed at 4 °C in ST buffer

supplemented with 10 μg leupeptin ml^{-1} and 50 μg L-tosyl lysyl chloromethyl ketone ml^{-1}. The cells were disrupted by 10 strokes in a Potter–Elvehiem homogenizer. The homogenate was diluted twice with ST buffer and centrifuged for 10 min at 700 ***g*** to remove the cell debris. The supernatant was spun for 10 min at 10 300 ***g***, resulting in a large granule fraction (sediment) and a crude cytosolic fraction (supernatant). The crude cytosolic fraction was centrifuged for 30 min at 140 000 ***g*** to obtain the final cytosolic fraction (supernatant) and microsomes in the sediment. The large granule fraction was loaded on a Percoll cushion (ST buffer containing 20 % Percoll; Amersham) and centrifuged for 30 min at 20 000 ***g*** to obtain hydrogenosomal and lysosomal fractions. Both fractions were washed twice with 10 vols ST buffer to remove the Percoll. All fractions were counted for total ^{59}Fe radioactivity and the protein content was assayed by the method of Lowry. Assays for marker enzymes [NAD-dependent malate dehydrogenase (decarboxylating), NADH oxidase and acid phosphatase)] were performed as described by Drmota *et al.* (1996), Rasoloson *et al.* (2002) and Müller (1973).

Kinetics of ^{59}Fe uptake. In a time-course experiment, 5×10^6 *Tt. foetus* cells were incubated with ^{59}Fe-NTA as described above in 250 μl NaCl-HEPES buffer for different time intervals (3–180 min). The parasites were immediately washed three times in ice-cold NaCl-HEPES buffer and stored at −70 °C.

In pulse–chase experiments, the cells (5×10^8) were incubated with ^{59}Fe-NTA as described above in 25 ml NaCl-HEPES buffer for 10 min. The parasites were washed three times in ice-cold NaCl-HEPES buffer to remove the unbound radioactivity and resuspended in 25 ml NaCl-HEPES buffer pre-warmed to 37 °C. The cell suspension was reincubated in the absence of radioactive iron for 0, 60 or 150 min at 37 °C, washed twice in ST buffer and the cells were immediately fractionated as described above.

Sample preparation, electrophoresis and storage phosphorimaging. Samples were solubilized by the addition of 20 % Triton X-100 to give a final detergent concentration of 1·5 % at 4 °C for 10 min. The lysates were vortexed and centrifuged at 4 °C for 20 min at 15 000 ***g***. Both pellets and supernatants were counted for ^{59}Fe radioactivity. Supernatants were then mixed with sample buffer (10 % sucrose with a trace amount of bromophenol blue stain) and aliquots corresponding to 500–2500 c.p.m. were applied to the sample wells for the electrophoretic separation. Protein load ranged from 20 to 600 μg per well. In the experiments focused on iron chelatability, DFO or Deferiprone was added to the samples prior to loading on the gel to give final Fe concentrations of 25, 100 or 500 μM.

Linear 3–20 % polyacrylamide gradient gels containing 1·5 % Triton X-100 were prepared for separation of iron-binding proteins as described by Vyoral *et al.* (1998). Separation of hydrogenosome-bound iron was performed using a 4–27 % linear polyacrylamide gradient to obtain better resolution at the front of the electrophoretogram. Electrophoresis was performed using a Hoeffer SE 600 vertical electrophoresis system with external cooling set to 4 °C at 110 mA constant current for two gel gradients. The electrode buffer contained 0·025 M Tris, 0·192 M glycine, pH 8·3. The run was stopped when haemoglobin, which was used as a marker, migrated to the middle of the gradient gel. The gels were then vacuum-dried, exposed to Storage Phophor Screen GP (Amersham) at room temperature for 24 h, scanned at a resolution of 100 μm per pixel using PhosphorImager SI (Amersham) and analysed using ImageQuantNT analysis software (Amersham). The dried gradient gels were rehydrated and stained in Coomassie brilliant blue solution after storage phosphorimaging analysis. After 2 days the stain was replaced by a solution containing 40 % methanol and 10 % acetic acid and the gels were destained overnight.

Molecular mass estimation of the LIP by ultrafiltration. The cytosolic fraction isolated from ^{59}Fe-NTA-labelled *Tt. foetus* cells (100 μl with a radioactivity of about 4000 c.p.m.) was added to 400 μl NaCl-HEPES buffer (140 mM NaCl, 10 mM HEPES, pH 7·2) and centrifuged at 5000 ***g*** for 90 min at 4 °C on Microcentrifuge Filters Ultrafree MC (Sigma) with the nominal molecular mass limits (NMML) of 5000 and 30 000 Da. The retentate was then washed twice with 200 μl NaCl-HEPES buffer. The washed retentates and the pooled ultrafiltrates were counted for ^{59}Fe radioactivity. When DFO-chelatable iron was assayed, the chelator was added to the mixture at a final concentration of 500 μM and the samples were processed as described above.

Atomic absorption spectrophotometry. Samples of cell fractions were diluted in cold PBS-chelex 100 (Sigma), sonicated and then analysed using a graphite furnace atomic absorption spectrophotometer model AS 800 (Perkin Elmer) at a wavelength of 248·3 nm with a 0·2 nm slit width and 20 mA lamp current. The following times and temperatures were used: injection at 80 °C; drying at 130 °C for 30 s with a 15 s ramp; charring at 1000 °C for 20 s with a 10 s ramp and atomization at 2450 °C for 3 s. The peak area was integrated for 10 s.

Amino acid sequencing. The major hydrogenosomal iron-binding protein was cut out from a rehydrated native gradient gel, separated by SDS-PAGE and transferred to a PVDF membrane. The band of interest was excised and submitted for amino-terminal sequence determination using Edman degradation at the Department of Biochemistry, Charles University, Faculty of Science, Prague, Czech Republic.

Cloning and screening of the genomic library. To obtain a probe for screening of a *Tt. foetus* genomic library (λ ZAP II; Stratagene), specific primers were designed (5′-TTCGGATCAATCGTCGG-3′ and 5′-TTGGAATGTAGCACCGT-3′) based on a partial *Tt. foetus* ferredoxin sequence found in the GenBank database under accession no. AF312935. The PCR-amplified fragment was cloned into a pCR 2.1 vector (TOPO TA Cloning kit; Invitrogen). The insert was excised from the vector, gel-purified and labelled by means of a Random Primer DNA Labelling System (Gibco-BRL) with [α-^{32}P]dATP. The sequences of positive clones were determined on both strands by primer walking. The consensus sequence of *Tt. foetus* ferredoxin (accession no. AF545472) was aligned to sequences of adrenodoxin-type ferredoxins from 42 taxa extracted from GenBank using CLUSTAL X (Thompson *et al.*, 2000) and further edited using BIOEDIT (Hall, 1999). A sequence identity matrix was calculated based on the alignment from which all gaps were removed using BIOEDIT.

RESULTS

Incorporation of iron from various sources into LIP

When incubated with ^{59}Fe-NTA, ^{59}Fe-lactoferrin or ^{59}Fe-transferrin, *Tt. foetus* incorporated the majority of the ^{59}Fe from all three sources into LIP. On electrophoretograms of the whole-cell lysates, iron associated with LIP was observed as a diffuse, rapidly migrating band (Fig. 1a). To verify that this band represents a chelatable pool of iron, two iron chelators (Deferiprone and DFO) were tested. Addition of both chelators to the ^{59}Fe-NTA-labelled cell lysate prior to electrophoresis resulted in concentration-dependent removal of the diffuse LIP band (Fig. 2). In the case of DFO, two residual bands appeared on the autoradiogram

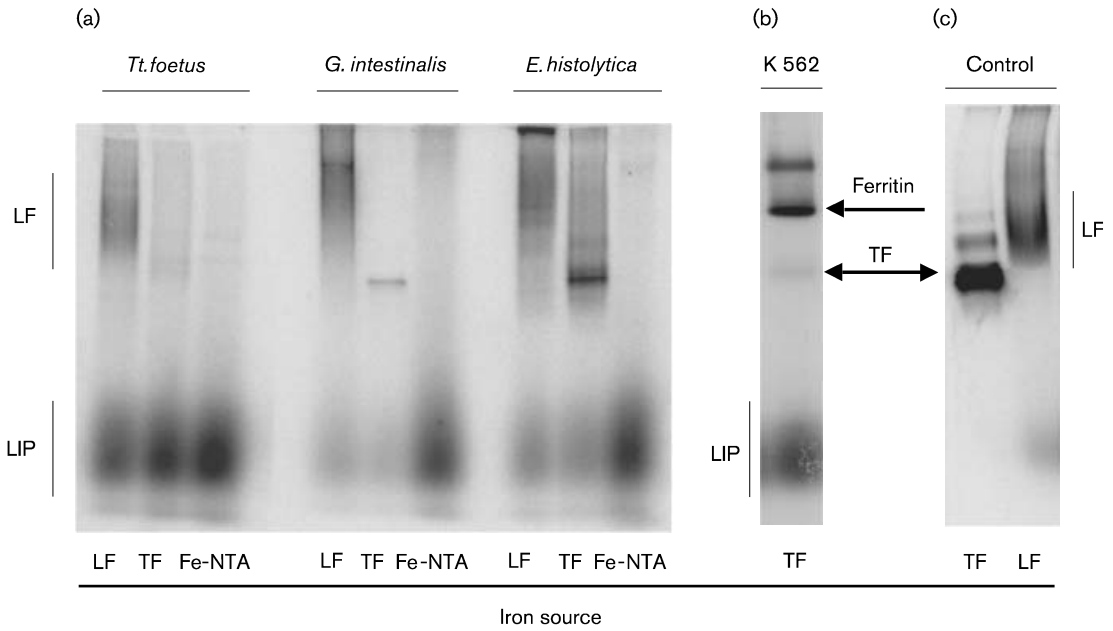

Fig. 1. Incorporation of iron from ^{59}Fe-NTA, ^{59}Fe-transferrin (TF) and ^{59}Fe-lactoferrin (LF) into the cells of *Tt. foetus*, *G. intestinalis* and *E. histolytica*. (a) The cells were incubated in the presence of ^{59}Fe-NTA, ^{59}Fe-transferrin or ^{59}Fe-lactoferrin at 37 °C for 60 min. Concentrations of iron corresponded to 150 ng ^{59}Fe ml^{-1}. Bovine transferrin and lactoferrin were used in experiments with *Tt. foetus*, while human proteins were used for the other two parasites. After the incubation, the cell lysates (1200 c.p.m. were loaded into each well) were analysed by native gradient PAGE and iron-containing compounds were detected by storage phosphorimaging. (b) K562 human leukaemic cells were incubated in the presence of human ^{59}Fe-transferrin and analysed as described above. (c) ^{59}Fe-labelled human transferrin and lactoferrin were used as controls.

(Fig. 2) which corresponded to ^{59}Fe-DFO complexes (Vyoral & Petrák, 1998a). In addition to LIP, lactoferrin-bound iron was observed in the cells incubated with ^{59}Fe-lactoferrin, which formed a slowly migrating diffuse band of the same mobility as the cell-free control samples (Fig. 1c). When trichomonads were incubated with ^{59}Fe-transferrin, the band corresponding to transferrin-bound iron was not observed in the cell lysates, although the parasites incorporated iron from transferrin into LIP (Fig. 1a). The latter observation is in agreement with an extracellular release of iron from transferrin without specific binding of transferrin to the cell surface (Tachezy *et al.*, 1996).

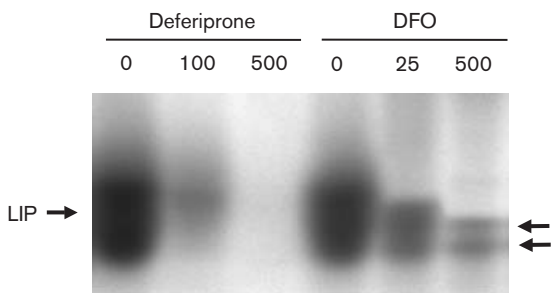

Fig. 2. Chelation of cellular LIP by Deferiprone and DFO. Samples of ^{59}Fe-NTA-labelled *Tt. foetus* cell lysate containing 3000 c.p.m. were mixed with different concentrations of Deferiprone or DFO and subjected to electrophoretic separation as described in Methods. Arrows indicate a residual double band after treatment with DFO corresponding to ^{59}Fe-chelator complexes.

Iron incorporation by *Tt. foetus* was then compared with that of two intestinal parasites, *G. intestinalis* and *E. histolytica* (Fig. 1a). Both parasites were able to incorporate iron from ^{59}Fe-NTA into LIP efficiently. When the intestinal parasites were incubated with Fe-lactoferrin or Fe-transferrin, a considerably lower incorporation of iron into LIP was observed. To test whether incorporation of iron into LIP from Fe-NTA, lactoferrin and transferrin reflects the ability of the cells to cover their nutritional requirements from corresponding iron sources, we compared the effect of Fe-NTA, lactoferrin and transferrin on the growth of the parasite *in vitro*. All three iron sources stimulated growth of *Tt. foetus*, while growth of *G. intestinalis* and *E. histolytica* was only stimulated by Fe-NTA (Table 1) and other low-molecular-mass iron complexes (data not shown). These observations suggest that LIP represents a physiologically important pool of intracellular iron associated with cell growth.

Incorporation of iron from Fe-NTA by parasitic protists was further compared with K562 human leukaemic cells (Fig. 1b). Unlike the parasites, K562 cells incorporated a significant part of intracellular iron into ferritin (about

Table 1. *In vitro* stimulation of *Tt. foetus*, *G. intestinalis* and *E. histolytica* growth by different iron-containing substances in Fe-depleted media

Iron-depleted medium was supplemented with a serial dilution of Fe-NTA, Fe-transferrin and Fe-lactoferrin in concentrations corresponding to 3·1–100 μM Fe. Values are means of at least six determinations.

Organism	Iron concentration for 50 % growth (μM)*		
	Fe-NTA	Fe-transferrin	Fe-lactoferrin
Tt. foetus	25	5	9
G. intestinalis	28	–	–
E. histolytica	50	–	–

*The concentration of iron required for stimulation of cell growth to 50 % of its maximal yield at an excess of iron (Tachezy *et al.*, 1996). The cell density at the maximal yield was 7×10^6, 5×10^6 and 1×10^6 for *Tt. foetus*, *G. intestinalis* and *E. histolytica*, respectively.

27 %). No major protein of parasite origin that binds iron with an intensity comparable to ferritin was observed in either *Tt. foetus* or the intestinal parasites (Fig. 1a).

Molecular mass estimation of LIP by ultrafiltration

^{59}Fe-NTA-labelled *Tt. foetus* was homogenized and the soluble fraction was used for ultrafiltration. As is apparent from Table 2, 7·6 % of the total sample radioactivity appeared in the ultrafiltrate when a 5000 NMML filter was used, whereas 68·3 % of the radioactivity was detected in the 30 000 NMML ultrafiltrate. Less then 22 % of LIP-bound iron was present in the 30 000 retenate. Addition of 500 μM DFO to the control sample before ultrafiltration resulted in an increase of radioactivity in the 5000 NMML ultrafiltrate to 95·1 %, whereas radioactivity detected in the retentate corresponded to only 4·9 %. These results indicate that only a small part of LIP is associated with low-molecular-mass iron complexes (<5000 Da), while the majority of LIP consists of compounds corresponding to the molecular mass range 5000–30 000 Da.

Table 2. Molecular mass estimation of LIP in *Tt. foetus* cytoplasm by an ultrafiltration assay

The samples were ultrafiltrated using membranes with an NMML of 5000 and 30 000 Da. ND, Not determined.

Sample	^{59}Fe (% c.p.m.)	
	5000 NMML	30 000 NMML
Cytosol		
Retentate	87·4	21·8
Filtrate	7·6	68·3
Cytosol + 500 μM DFO		
Retentate	4·9	ND
Filtrate	95·8	ND

Iron in the cell fractions

First we investigated the steady-state level of iron during long-term cultivation of *Tt. foetus* in complex TYM medium. Iron concentrations were determined using atomic absorption spectrophotometry in two cell fractions, cytosol and hydrogenosomes, isolated from the cells during the exponential growth phase. This determination revealed an unusually high iron concentration in *Tt. foetus* hydrogenosomes [$54{\cdot}4 \pm 1{\cdot}1$ nmol Fe (mg protein)$^{-1}$; $n=3$], which was fourfold higher than that in cytosol [$13{\cdot}4 \pm 0{\cdot}5$ nmol Fe (mg protein)$^{-1}$; $n=6$]. The iron content determined in the TYM media was $19{\cdot}7 \pm 0{\cdot}05$ μM ($n=3$).

In other experiments, we investigated iron incorporation and its subcellular distribution when the trichomonads were incubated in a simple NaCl-HEPES buffer for 1 h with ^{59}Fe-NTA. Four cell fractions were isolated (cytosol, hydrogenosomes, lysosomes and microsomes) and the incorporated radioactivity was determined for each fraction (Fig. 3). The majority of the iron (88·9 %) was present in the cytosol. The cytosolic iron concentration calculated from incorporated radioactivity was 304·7 pmol ^{59}Fe (mg protein)$^{-1}$. The hydrogenosomes possessed only 4·7 % of the total incorporated radioactivity; however, the iron concentration was the highest as compared to other cell compartments [360·4 pmol ^{59}Fe (mg protein)$^{-1}$]. Lysosomes and microsomes contained only 2·9 and 3·4 % of the total incorporated radioactivity, respectively. These results showed iron to be efficiently taken up and transported to the hydrogenosomes by *Tt. foetus*.

Remarkable differences were observed in the solubilization of incorporated radioactive iron in 1·5 % Triton X-100. When Triton X-100 was added to whole-cell lysate, cytosol and microsomes, about 81, 100 and 79 % of the total radioactivity was found in the solubilized fraction, respectively. However, addition of the detergent to hydrogenosomes and lysosomes released only 26 and 30 % of radioactive iron into the supernatant, respectively, while the majority of the iron was pelleted. The supernatants were further used for electrophoretic analysis (Fig. 4a). In the cytosol, a prominent band designated 'C' and at least four additional bands containing ^{59}Fe were observed. The majority of iron was present in LIP (about 62 %). The band pattern of the cytosolic fraction was similar to that observed in the whole-cell lysate. However, a remarkably different pattern was displayed by the hydrogenosomes. A prominent fast-migrating band (H-I) was observed within these organelles as well as eight other bands which differed in mobility from those found in the cytosol. In microsomes and lysosomes we observed only weak bands, which were at the detection limit of our assay. The H-I band, as well as other bands in the hydrogenosomes, correspond to hydrogenosomal FeS proteins such as PFOR, ferredoxin and

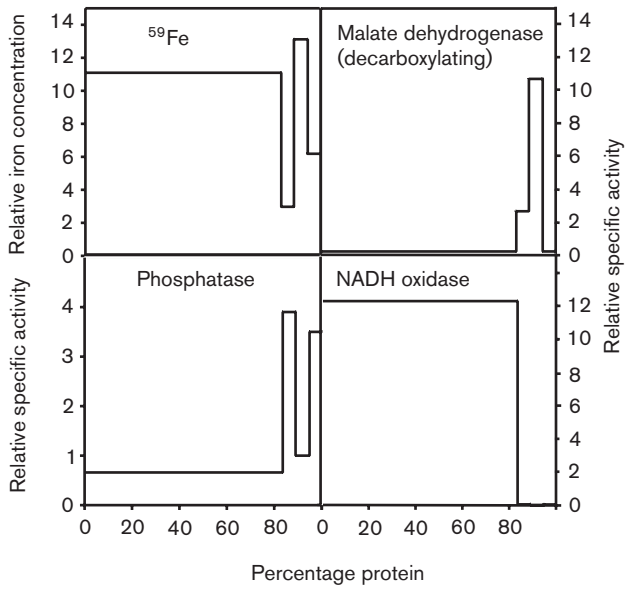

Fig. 3. Distribution of iron incorporated from ^{59}Fe-NTA into the subcellular fractions of *Tt. foetus*. *Tt. foetus* cells were incubated in the presence of ^{59}Fe-NTA (150 ng ^{59}Fe ml^{-1}) at 37 °C for 60 min. After the incubation, the cells were washed, disrupted and four subcellular fractions were obtained by means of differential and Percoll gradient centrifugation: cytosol, microsomes, hydrogenosomes and lysosomes. The total radioactivity in the fractions was determined by a γ-counter and protein content was assayed according to the method of Lowry. Relative ^{59}Fe radioactivity was plotted against cumulative percentage of protein recovered in each fraction. The order of the fractions from the left is: cytosol, lysosomes, hydrogenosomes and microsomes. NADH oxidase, acid phosphatase and NAD-dependent malate dehydrogenase (decarboxylating) were used as marker enzymes for cytosol, hydrogenosomes and lysosomes, respectively.

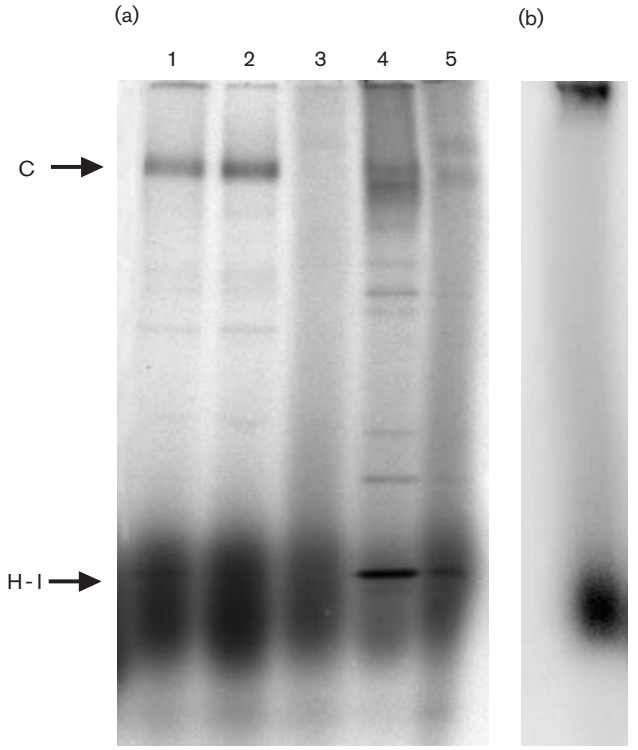

Fig. 4. Incorporation of iron from ^{59}Fe-NTA into the subcellular fractions of *Tt. foetus*. The *Tt. foetus* metronidazole-sensitive strain Lub-1 MIP or metronidazole-resistant strain Lub-1 MR100 were incubated at 37 °C for 60 min in the presence of ^{59}Fe-NTA (150 ng ^{59}Fe ml^{-1}). After incubation, the cells were immediately fractionated by means of differential and Percoll gradient centrifugation. The samples containing about 3000 c.p.m. were loaded into each well and analysed by native gradient PAGE followed by storage phosphorimaging. (a) Lub-1 MIP strain. Lanes: 1, whole-cell lysate; 2, cytosol; 3, microsomes; 4, hydrogenosomes; 5, lysosomes. (b) Lub-1 MR100 strain hydrogenosomes.

hydrogenase. As these proteins are absent in metronidazole-resistant strains (Rasoloson *et al.*, 2002), we compared iron incorporation into hydrogenosomes of a metronidazole-sensitive strain (Lub-1MIP) and its resistant derivative (Lub-MR100). Indeed, none of the eight bands present in the parent strain was observed in the resistant derivative (Fig. 4b).

Kinetics of iron incorporation

Two types of experiments were used to study the kinetics of iron incorporation into *Tt. foetus*. In time-course experiments, cells were incubated for 3–180 min and whole-cell lysates were separated electrophoretically (Fig. 5). Cytosolic band C appeared at the shortest time interval (3 min) and its intensity increased during prolonged incubation. Appearance of the hydrogenosomal H-I band was delayed from band C for at least 60 min. The intensity of the H-I band also increased in a time-dependent manner. In pulse–chase experiments, trichomonads were incubated for 10 min with ^{59}Fe-NTA and then reincubated without radioactive iron for 0, 60 and 150 min. At each time point, the cells were fractionated and the cellular fractions were analysed as described above (Fig. 6). The intensity of all cytosolic bands increased during the cell reincubation, indicating that all observed cytosolic bands represent a final destination of iron transport. In hydrogenosomes, the intensity of the H-I band did not significantly change during reincubation. A remarkable increase in bound radioactivity was observed in the slower migrating band H-II. We also observed a single band (H-III), which was present after the 10 min incubation of cells with ^{59}Fe-NTA and disappeared during cell reincubation. The kinetics of the H-III band suggest its role as an intermediate involved in iron transport.

Analysis of the H-I band

The H-I band appeared as a major iron-binding compound in hydrogenosomes (Figs 4a and 6). The H-I-associated iron

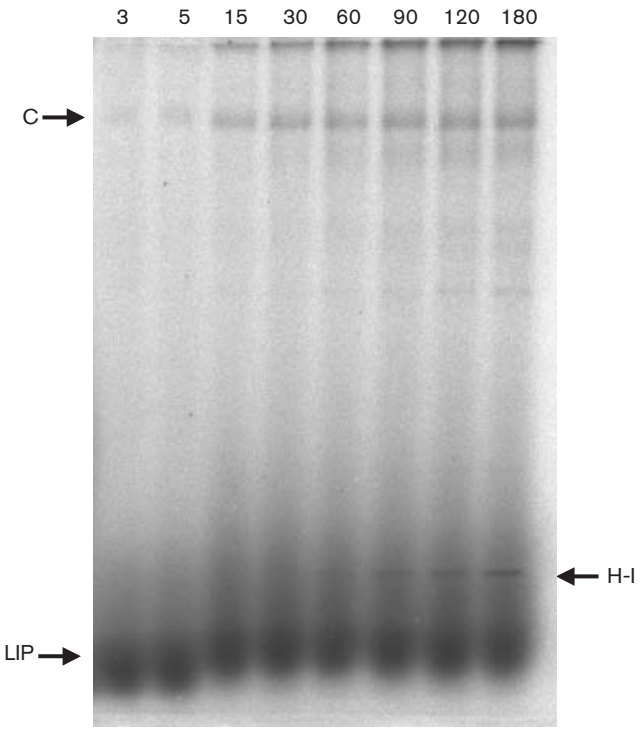

Fig. 5. Kinetics of iron uptake during time-course experiments. *Tt. foetus* cells were incubated with ^{59}Fe-NTA for 3, 5, 15, 30, 60, 90, 120 or 180 min. The parasites were subsequently washed and the cell lysates were analysed by native gradient PAGE. Samples containing 1000 c.p.m. were loaded into each well, the gel was dried after electrophoresis and iron-containing compounds were detected by storage phosphorimaging.

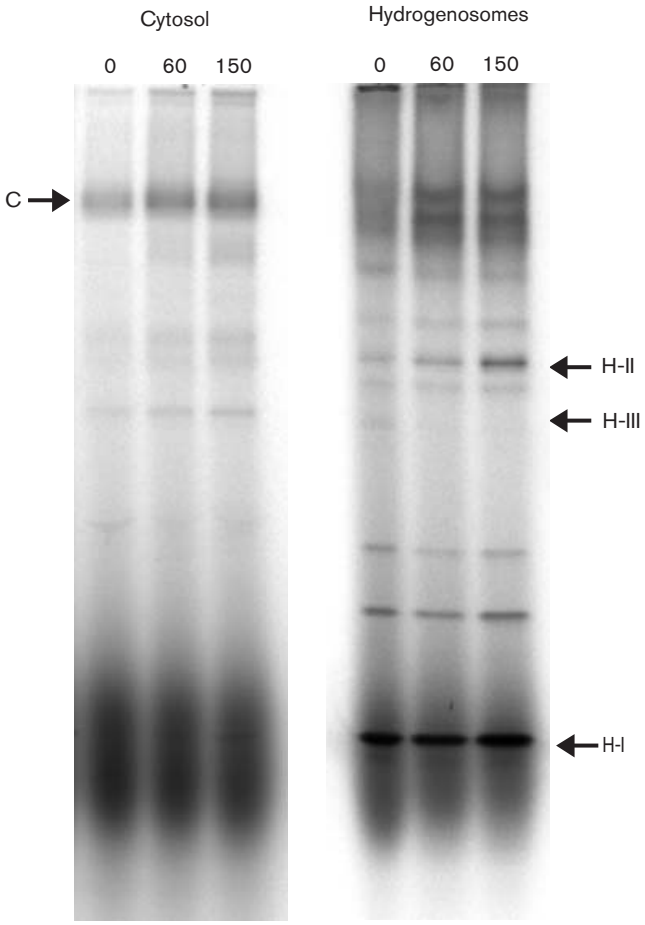

Fig. 6. Kinetics of iron uptake in pulse–chase experiments. Cells were incubated with ^{59}Fe-NTA for 10 min, washed and reincubated in the absence of radioactive iron for 0, 60 or 150 min at 37 °C. Cytosolic and hydrogenosomal fractions obtained by means of differential and Percoll gradient centrifugation were analysed by native gradient PAGE followed by storage phosphorimaging (3000 c.p.m. per well).

was rather tightly bound, as it was not removed by 500 μM DFO (Fig. 7). To estimate the molecular mass of the compound corresponding to the H-I band, the native gradient gel was rehydrated after autoradiography and stained by Coomassie brilliant blue. The band of corresponding mobility was cut-out and separated by SDS-PAGE which showed the presence of a 12 kDa protein (data not shown). This protein was submitted to Edman degradation to determine the N-terminal sequence. A sequence of 29 aa was obtained which matched exactly the N-terminal part of *Tt. foetus* ferredoxin as predicted from the partial gene sequence in GenBank. A complete *Tt. foetus* ferredoxin gene was subsequently obtained by screening of a *Tt. foetus* genomic library. Sequence analysis of the ferredoxin gene revealed an ORF of 327 bp, encoding 109 aa. The molecular mass and isoelectric point were 11 052 Da and 4·48, respectively. The N terminus of the predicted *Tt. foetus* ferredoxin contained a 13 aa extension similar to presequences known to target the proteins to hydrogenosomes in *T. vaginalis* (Bradley *et al.*, 1997; Johnson *et al.*, 1990). This extension was absent from the N-terminal sequence of the isolated peptide, indicating that the ferredoxin presequence had been processed within the *Tt. foetus* hydrogenosomes. Presence of a conserved $CX_5CX_2CX_nC$ pattern indicated that the ferredoxin belongs to the [2Fe–2S] adrenodoxin type found in other amitochondrial protists, mitochondria of eukaryotes and bacteria (Fig. 8). Comparison of the *Tt. foetus* ferredoxin with 42 sequences of adrenodoxin-type ferredoxins found in databases revealed the highest identity in a 66 aa overlap with the ferredoxin of *T. vaginalis* (58 %) and *G. intestinalis* (33 %), and with mitochondrial-type ferredoxin of *Saccharomyces cerevisiae*, *Mus musculus* and *Caenorhabditis elegans* (29–33 %). Significant similarity was also found in the proteobacterial ferredoxin of *Acinetobacter* sp. (33 %) and the cyanobacterium *Mastigocladus laminosus* (32 %). An alignment of selected homologues is shown in Fig. 8 (the complete alignment is available on request). These data show that a ferredoxin of the adrenodoxin type is a major iron-binding protein in the hydrogenosomes of *Tt. foetus*.

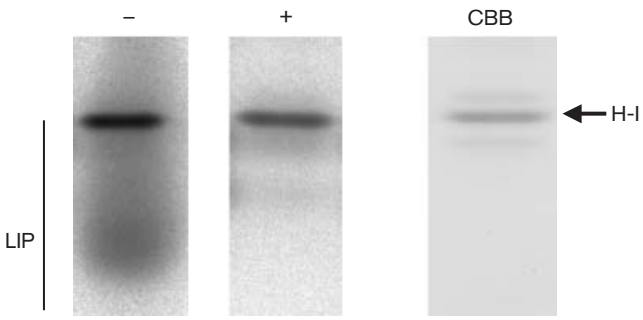

Fig. 7. Stability of hydrogenosomal H-I band-associated iron in the presence of the iron chelator. The hydrogenosomal fractions isolated from ^{59}Fe-NTA-labelled *Tt. foetus* containing 3000 c.p.m. were incubated in the absence (–) or presence (+) of 500 μM DFO before loading on the gels and were analysed by electrophoresis as described in Methods. After autoradiography, the gel was rehydrated and stained with Coomassie brilliant blue (CBB).

DISCUSSION

In this work we studied the incorporation of iron by *Tt. foetus* using native gradient PAGE followed by storage phosphorimaging. This method allowed the direct monitoring of iron incorporation into cell fractions. In the cytosol, the majority of iron was incorporated into LIP, while in the hydrogenosomes, a major iron-binding protein was identified as a [2Fe–2S] ferredoxin of the adrenodoxin type.

The molecular basis and physiological significance of LIP has been an enigma for decades. It is believed to be an iron transport intermediate in iron acquisition from the cellular environment. It is also hypothesized to be involved in iron mobilization from its intracellular storage (Crichton, 1991). However, kinetics studies of LIP in K562 cells showed the chelatable compartment of cellular iron to be labelled with the kinetics of an end product (Vyoral & Petrák, 1998b), which argues against an intermediate character of LIP. It has been suggested that the 'mobile' iron forms low-molecular-mass complexes with nucleotides, nucleic acids, polyphosphates, amino acids, citrate or peptides (Jacobs, 1977; Bohnke & Matzanke, 1995; Weaver & Pollack, 1989). However, increasing evidence indicates that 'mobile' iron is (with low affinity) bound to compounds most likely to be proteins with a molecular mass greater than 20 000 Da (Petrák & Vyoral, 2001; Vyoral & Petrák, 1998a, b; Vyoral *et al.*, 1992). This view is supported by our results using ultrafiltration of iron-labelled cytosol of *Tt. foetus*. It showed that 68·2 % of chelatable iron is bound to compounds with a molecular mass in the range of 5000–30 000 Da. Thus, it is likely that LIP in protists represents low-affinity iron associated with housekeeping proteins. The importance of LIP for cell function is supported by our observation that its presence correlated with the ability of cells to utilize various iron sources for their growth. The difference between LIP in protists and vertebrate cells is its abundance. In various human cell lines the LIP band corresponded to 5–30 % of cellular iron, while a greater part of intracellular iron is stored in ferritin (Vyoral *et al.*, 1998). In protists, which do not possess ferritin, >60 % of iron appeared as chelation-sensitive LIP.

It is noteworthy that neither *Tt. foetus* nor other unicellular eukaryotes possesses ferritin. Higher eukaryotes rely on ferritin to scavenge and to store iron in the cytosol. Recently, ferritin has also been found in mitochondria (Levi *et al.*, 2001), although the function of mitochondrial ferritin remains to be clarified. Two types of ferritin are present in bacteria, including the α-proteobacteria (Andrews *et al.*, 1991), which are considered to be the endosymbiotic ancestors of mitochondria and hydrogenosomes (Rotte *et al.*, 2000; Dyall & Johnson, 2000). In three parasitic protists, we were unable to detect any protein of comparable mobility and iron-binding capacity with ferritin observed in K562 cells. The presence of a ferritin-encoding gene has not been reported in any unicellular eukaryote so far with the exception of the microsporidian parasite *Encephalitozoon cuniculi* (Katinka *et al.*, 2001).

Hydrogenosomes represent an important destination of intracellular iron and this is supported by the following evidence: (i) iron is required for the catalytic centres of FeS proteins such as PFOR, ferredoxin and hydrogenase, which mediate key steps in hydrogenosomal pyruvate metabolism

```
T.foetus         MALSFPSQSF RRFGSIVGIT KGGEKKTIEF EDDQNLFELL TGAGVISPEG  50
T.vaginalis      -----MLSQV CRFGTITAV- KGGVKKQLKF EDDQTLFTVL TEAGLMSADD  44
G.intestinalis   ----MSLLSS IRRFITFRVV QQGVEHTVSG AVGQSLLDAI KAAH-IPIQD  45
S.cerevisiae     ML(X)59KPKP GEELKITFIL KDGSQKTYEV CEGETILDIA QGHN-LDMEG  45
E.coli           ------MPKI VILPHQD-LC PDG--AVLEA NSGETILDAA LRNG-IEIEH  40

T.foetus         TCNGNVACGK CLVKVVSG-- -NVAAAEDEE KELLD---GA PAGARLACAI  94
T.vaginalis      TCQGNKACGK CICKHVSG-- --KVAAEDDE KEFLE---DQ PANARLACAI  87
G.intestinalis   ACEGHLXCGT CGVYLDKKTY KRIPRATKEE AVLLDQVPNP KPTSRLSCAV  95
S.cerevisiae     ACGGSCACST CHVIVDPDYY DALPEPEDDE NDMLDLAYGL TETSRLGCQI  95
E.coli           ACEKSCACTT CHCIVREG-F DSLPESSEQE DDMLDKAWGL EPESRLSCQA  89

T.foetus         SLDSGANGAT FQAL------ ---------- -------- 108
T.vaginalis      TLSGENDGAV FEL------- ---------- -------- 100
G.intestinalis   KLSSMLEGAT VRIPSFNKNV LSESDILASE EKKRHGQH 133
S.cerevisiae     KMSKDIDGIR VALPQMTR-N VNNNDFS--- -------- 121
E.coli           RVTD--EDLV VEIPRYTINH AREH------ -------- 111
```

Fig. 8. Alignment of *Tt. foetus* ferredoxin (AF545472) to [2Fe–2S] ferredoxins of amitochondrial protists *T. vaginalis* (A36003) and *G. intestinalis* (AAL95709), adrenodoxin of *S. cerevisiae* (NP 015071) and *Escherichia coli* ferredoxin from the *isc* gene cluster (P25528). The arrow indicates a putative cleavage site of the *Tt. foetus* ferredoxin leader sequence. The sequence determined by Edman degradation is underlined. Conserved cysteines coordinating the [2Fe–2S] cluster are boxed.

(Vaňáčová *et al.*, 2001); (ii) hydrogenosomes efficiently accumulated iron when the trichomonads were incubated with ^{59}Fe-NTA [360·4 pmol ^{59}Fe h^{-1} (mg protein)$^{-1}$]; and (iii) the steady-state concentration of iron in hydrogenosomes was about fourfold higher than that in cytosol as determined by atomic absorption spectrophotometry. The iron content in hydrogenosomes [54·4 nmol Fe (mg protein)$^{-1}$] is unusually high. In yeast the concentrations of mitochondrial iron range from 0·512 to 4·9 nmol (mg mitochondrial protein)$^{-1}$ when the organisms are grown on media containing 0·1–50 μM Fe (Li *et al.*, 1999). A similar level of iron has been also found in mammalian mitochondria (Tangeras, 1985). Mitochondrial iron concentrations comparable to that in hydrogenosomes have only been observed in yeast mutants with altered iron homeostasis (Li *et al.*, 1999).

The iron retained in hydrogenosomes consists of Triton X-100-soluble (26 %) and -resistant fractions (74 %). In yeast mitochondria, the Triton X-100-resistant fraction formed only a small proportion of total iron (5–12 %); however, it increased to 53–60 % in mutants with altered iron homeostasis (Li *et al.*, 1999). It has been suggested that pelleted iron represents the iron pool associated with membrane lipids or protein aggregates (Li *et al.*, 1999). However, its biological function is not known. The high proportion of Triton X-100-resistant iron in hydrogenosomes together with the absence of ferritin suggests that this iron may represent intrahydrogenosomal iron storage. The solubilized iron appeared as distinct bands on autoradiograms. It is likely that the bands correspond mainly to FeS proteins involved in pyruvate metabolism (PFOR, hydrogenase, ferredoxin) as they were absent in hydrogenosomes of metronidazole-resistant trichomonads. Decreased expression of hydrogenosomal proteins, including PFOR and ferredoxin, in metronidazole-resistant strains was recently reported in *T. vaginalis* (Rasoloson *et al.*, 2002) and *Tt. foetus* (Land *et al.*, 2001). The major iron-containing protein was isolated and identified as [2Fe–2S] ferredoxin. DFO, chelating non-specifically or weakly bound iron, did not remove radioactive iron associated with the labelled ferredoxin. This observation indicated that ^{59}Fe was specifically incorporated into this protein, most likely into the chelation-resistant FeS centre. Moreover, chemical analysis of ferredoxin from a related organism, *T. vaginalis*, revealed approximately equal amounts of iron and acid-labile sulfur (Gorrell *et al.*, 1984). The function of ferredoxin in hydrogenosomal metabolism is well established and the protein has been biochemically characterized (Marczak *et al.*, 1983; Gorrell *et al.*, 1984). It is considered as a major electron carrier providing reducing equivalents to hydrogenase, which results in the formation of molecular hydrogen (Kulda, 1999; Martin & Müller, 1998). Molecular analysis of *T. vaginalis* ferredoxin showed closest similarity to putidaredoxin of *Pseudomonas putida* and to a lesser extent to mitochondrial [2Fe–2S] ferredoxins (adrenodoxins) of vertebrates, which are components of mixed-function oxidase systems (Johnson *et al.*, 1990). More recently, a different function was suggested for adrenodoxin-type ferredoxins. Genetic studies showed that adrenodoxin (Yah1p) is essential for the maturation of FeS proteins in yeast mitochondria (Lange *et al.*, 2000). The homologues of adrenodoxins are ferredoxins encoded in the bacterial *isc* gene cluster together with other components of FeS cluster assembly machinery such as IscS, IscU and IscA (Takahashi & Nakamura, 1999). Adrenodoxins, as well as their bacterial homologues, form a group of [2Fe–2S] ferredoxins with a common cluster-binding pattern, $CX_5CX_2CX_nC$ (Bertini *et al.*, 2002). As is apparent from primary structure analysis, [2Fe–2S] ferredoxin present in the amitochondrial protists *Tt. foetus*, *T. vaginalis* and *G. intestinalis* (Nixon *et al.*, 2002) belongs to the adrenodoxin group (this study; Johnson *et al.*, 1990; Land *et al.*, 2002). The genes for a key component of FeS cluster assembly machinery, IscS, have been recently found both in trichomonad species and in *G. intestinalis* (Tachezy *et al.*, 2001), indicating that common mechanisms of FeS protein biogenesis operate in mitochondrial as well as amitochondrial eukaryotes. Thus, it is likely that hydrogenosomal ferredoxin, in addition to its known metabolic function, is also involved in FeS cluster formation. The exact role of ferredoxin in this process is not known. Lange *et al.* (2000) suggested that ferredoxin may provide reducing equivalents for the formation of FeS cluster intermediates, which are pre-assembled on NifU/IscU or IscA proteins serving as a scaffold. Ollagnier-de-Choudens *et al.* (2001) showed that FeS intermediates formed on IscA are delivered to ferredoxin, and proposed that this process is a key step in the biosynthesis of the FeS cluster required for maturation of other cellular FeS proteins. The abundance of ferredoxin in *Tt. foetus* hydrogenosomes supports the latter possibility. It is tempting to speculate that ferredoxin represents a pool of pre-assembled FeS clusters that are provided during biogenesis of other hydrogenosomal FeS proteins.

This study raises a number of intriguing questions such as: (i) how is iron delivered to hydrogenosomes, and (ii) which species supply iron for FeS cluster formation in the organelles? The kinetic studies did not reveal any compound with the kinetics of a putative iron transporter in the cytosol. All cytosolic compounds were observed as distinct bands on autoradiograms with increasing intensity in a time-dependent manner. It is likely that these compounds represent the final destinations of iron transport. The putative intracellular iron transporter is either hidden in LIP or the iron might be transported in endosomal vesicles (Richardson *et al.*, 1996). The hydrogenosomal H-III band was the only band with a transient kinetic pattern. Such kinetic behaviour would be typical for an iron transporter.

In conclusion, we have examined the iron-binding compounds in *Tt. foetus* cell fractions using native gradient PAGE followed by storage phosphorimaging. Our results demonstrate that hydrogenosomes represent an important destination in cellular iron transport and contain an unusually high iron concentration. We also determined ferredoxin to be a major iron-binding protein in these organelles. LIP appeared as a physiologically important iron

pool, although its molecular basis remains enigmatic. The efficient iron accumulation and high concentrations of intracellular iron in *Tt. foetus* correspond to its high nutritional demands for this metal (Tachezy *et al.*, 1996) and to the importance of iron for the virulence of this parasite (Kulda *et al.*, 1998).

ACKNOWLEDGEMENTS

This work was supported by grants of the Grant Agency of the Czech Republic 204/00/1561 (J. T.), MSM 11310 0003, and a Fogarty International Research Collaboration Award (J. T.), and in part by the Research Grants 5003-4 (E. N.) and 6574-3 (D. V.) of the Grant Agency of the Ministry of Health of the Czech Republic. The authors would like to thank Dr D. J. Sullivan (Johns Hopkins University, Baltimore) for his support, Dr V. Culotta and Dr L. Jensen (Johns Hopkins University, Baltimore) for help with atomic absorption spectrophotometry, Dr Karel Bezouška (Faculty of Science, Charles University, Prague) for peptide microsequencing, and Dr A. Dancis (University of Pennsylvania, Philadelphia) and Dr M. Müller (The Rockefeller University, New York) for critical reading of the manuscript.

REFERENCES

Andrews, S. C., Smith, J. M. A., Yewdall, S. J., Guest, J. R. & Harrison, P. M. (1991). Bacterioferritins and ferritins are distantly related in evolution – conservation of ferroxidase-center residues. *FEBS Lett* **293**, 164–168.

Bates, G. W. & Wernicke, J. (1971). The kinetics and mechanism of iron(III) exchange between chelates and transferrin. *J Biol Chem* **246**, 3679–3685.

Bertini, I., Luchinat, C., Provenzani, A., Rosato, A. & Vasos, P. R. (2002). Browsing gene banks for Fe_2S_2 ferredoxins and structural modeling of 88 plant-type sequences: an analysis of fold and function. *Prot Struct Funct Genet* **46**, 110–127.

Bohnke, R. & Matzanke, B. F. (1995). The mobile ferrous iron pool in *Escherichia coli* is bound to a phosphorylated sugar derivative. *Biometals* **8**, 223–230.

Bradley, P. J., Lahti, C. J., Plümper, E. & Johnson, P. J. (1997). Targeting and translocation of proteins into the hydrogenosome of the protist *Trichomonas*: similarities with mitochondrial protein import. *EMBO J* **16**, 3484–3493.

Brown, D. M., Upcroft, J. A., Edwards, M. R. & Upcroft, P. (1998). Anaerobic bacterial metabolism in the ancient eukaryote *Giardia duodenalis*. *Int J Parasitol* **28**, 149–164.

Crichton, R. (1991). Intracellular iron storage – ferritin, haemosiderin and the low molecular weight iron pool. In *Inorganic Biochemistry of Iron Metabolism*, pp. 131–162. New York: Ellis Horwood.

Diamond, L. S. (1957). The establishment of various trichomonads of animals and man in axenic cultures. *J Parasitol* **43**, 488–490.

Diamond, L. S., Harlow, W. D. & Cunnick, C. C. (1978). A new medium for the axenic cultivation of *Entamoeba histolytica* and other *Entamoeba*. *Trans R Soc Trop Med Hyg* **72**, 431–432.

Drmota, T., Proost, P., Van Ranst, M., Weyda, F., Kulda, J. & Tachezy, J. (1996). Iron-ascorbate cleavable malic enzyme from hydrogenosomes of *Trichomonas vaginalis*: purification and characterization. *Mol Biochem Parasitol* **83**, 221–234.

Dyall, S. D. & Johnson, P. J. (2000). Origins of hydrogenosomes and mitochondria: evolution and organelle biogenesis. *Curr Opin Microbiol* **3**, 404–411.

Ellis, J. E., Williams, R., Cole, D., Cammack, R. & Lloyd, D. (1993). Electron transport components of the parasitic protozoon *Giardia lamblia*. *FEBS Lett* **325**, 196–200.

Gorrell, T. E. (1985). Effect of culture medium iron content on biochemical composition and metabolism of *Trichomonas vaginalis*. *J Bacteriol* **161**, 1228–1230.

Gorrell, T. E., Yarlett, N. & Müller, M. (1984). Isolation and characterization of *Trichomonas vaginalis* ferredoxin. *Carlsberg Res Commun* **49**, 259–268.

Hall, T. A. (1999). BioEdit: a user-friendly biological sequence alignment editor and analysis program for Windows 95/98/NT. *Nucleic Acids Symp Ser* **41**, 95–98.

Jacobs, A. (1977). Low molecular weight intracellular iron transport compounds. *Blood* **50**, 433–439.

Johnson, P. J., d'Oliveira, C. E., Gorrell, T. E. & Müller, M. (1990). Molecular analysis of the hydrogenosomal ferredoxin of the anaerobic protist *Trichomonas vaginalis*. *Proc Natl Acad Sci U S A* **87**, 6097–6101.

Katinka, M. D., Duprat, S., Cornillot, E. & 14 other authors (2001). Genome sequence and gene compaction of the eukaryote parasite *Encephalitozoon cuniculi*. *Nature* **414**, 450–453.

Keister, D. B. (1983). Axenic culture of *Giardia lamblia* in TYI-S-33 medium supplemented with bile. *Trans R Soc Trop Med Hyg* **77**, 487–488.

Kulda, J. (1999). Trichomonads, hydrogenosomes and drug resistance. *Int J Parasitol* **29**, 199–212.

Kulda, J., Poislová, M., Suchan, P. & Tachezy, J. (1998). Enhancing effect of iron on experimental infection of mice by *Tritrichomonas foetus*. *Parasitology* **85**, 692–699.

Land, K. M., Clemens, D. L. & Johnson, P. J. (2001). Loss of multiple hydrogenosomal proteins associated with organelle metabolism and high-level drug resistance in trichomonads. *Exp Parasitol* **97**, 102–110.

Land, K. M., Delgadillo, M. G. & Johnson, P. J. (2002). In vivo expression of ferredoxin in a drug resistant trichomonad increases metronidazole susceptibility. *Mol Biochem Parasitol* **121**, 153–157.

Lange, H., Kaut, A., Kispal, G. & Lill, R. (2000). A mitochondrial ferredoxin is essential for biogenesis of cellular iron-sulfur proteins. *Proc Natl Acad Sci U S A* **97**, 1050–1055.

Levi, S., Corsi, B., Bosisio, M., Invernizzi, R., Volz, A., Sanford, D., Arosio, P. & Drysdale, J. (2001). A human mitochondrial ferritin encoded by an intronless gene. *J Biol Chem* **276**, 24437–24440.

Li, J., Kogan, M., Knight, S. A., Pain, D. & Dancis, A. (1999). Yeast mitochondrial protein, Nfs1p, coordinately regulates iron-sulfur cluster proteins, cellular iron uptake, and iron distribution. *J Biol Chem* **274**, 33025–33034.

Lill, R. & Kispal, G. (2000). Maturation of cellular Fe–S proteins: an essential function of mitochondria. *Trends Biochem Sci* **25**, 352–356.

Marczak, R., Gorrell, T. E. & Müller, M. (1983). Hydrogenosomal ferredoxin of the anaerobic protozoon, *Tritrichomonas foetus*. *J Biol Chem* **258**, 12427–12433.

Martin, W. & Müller, M. (1998). The hydrogen hypothesis for the first eukaryote. *Nature* **392**, 37–41.

Mazurier, J. & Spik, G. (1980). Comparative study of the iron-binding properties of human transferrins. I. Complete and sequential iron saturation and desaturation of the lactotransferrin. *Biochim Biophys Acta* **629**, 399–408.

Müller, M. (1973). Biochemical cytology of trichomonad flagellates. I. Subcellular localization of hydrolases, dehydrogenases, and catalase in *Tritrichomonas foetus*. *J Cell Biol* **57**, 453–474.

Müller, M. (1988). Energy metabolism of protozoa without mitochondria. *Annu Rev Microbiol* **42**, 465–488.

Müller, M. (1993). The hydrogenosome. *J Gen Microbiol* **139**, 2879–2889.

Nixon, J. E. J., Wang, A., Morrison, H. G., McArthur, A. G., Sogin, M. L., Loftus, B. J. & Samuelson, J. (2002). A spliceosomal intron in *Giardia lamblia*. *Proc Natl Acad Sci U S A* **99**, 3701–3705.

Ollagnier-de-Choudens, S., Mattioli, T., Tagahashi, Y. & Fontecave, M. (2001). Iron–sulfur cluster assembly – Characterization of IscA and evidence for a specific and functional complex with ferredoxin. *J Biol Chem* **276**, 22604–22607.

Payne, M. J., Chapman, A. & Cammack, R. (1993). Evidence for an [Fe]-type hydrogenase in the parasitic protozoan *Trichomonas vaginalis*. *FEBS Lett* **317**, 101–104.

Peterson, K. M. & Alderete, J. F. (1984). Iron uptake and increased intracellular enzyme activity follow host lactoferrin binding by *Trichomonas vaginalis* receptors. *J Exp Med* **160**, 398–410.

Petrák, J. & Vyoral, D. (2001). Detection of iron-containing proteins contributing to the cellular labile iron pool by a native electrophoresis metal blotting technique. *J Inorg Biochem* **86**, 669–675.

Quon, D. V., d'Oliveira, C. E. & Johnson, P. J. (1992). Reduced transcription of the ferredoxin gene in metronidazole-resistant *Trichomonas vaginalis*. *Proc Natl Acad Sci U S A* **89**, 4402–4406.

Rasoloson, D., Tomková, E., Cammack, R., Kulda, J. & Tachezy, J. (2001). Metronidazole-resistant strains of *Trichomonas vaginalis* display increased susceptibility to oxygen. *Parasitology* **123**, 45–56.

Rasoloson, D., Vaňáčová, S., Tomková, E., Razga, J., Hrdý, I., Tachezy, J. & Kulda, J. (2002). Mechanisms of *in vitro* development of resistance to metronidazole in *Trichomonas vaginalis*. *Microbiology* **148**, 2467–2477.

Richardson, D. R., Ponka, P. & Vyoral, D. (1996). Distribution of iron in reticulocytes after inhibition of heme synthesis with succinylacetone: examination of the intermediates involved in iron metabolism. *Blood* **87**, 3477–3488.

Rotte, C., Henze, K., Müller, M. & Martin, W. (2000). Origins of hydrogenosomes and mitochondria – commentary. *Curr Opin Microbiol* **3**, 481–486.

Tachezy, J., Kulda, J., Bahníková, I., Suchan, P., Rázga, J. & Schrével, J. (1996). *Tritrichomonas foetus:* iron acquisition from lactoferrin and transferrin. *Exp Parasitol* **83**, 216–228.

Tachezy, J., Suchan, P., Schrével, J. & Kulda, J. (1998). The host–protein independent iron uptake by *Tritrichomonas foetus*. *Exp Parasitol* **90**, 155–163.

Tachezy, J., Sánchez, L. B. & Müller, M. (2001). Mitochondrial type iron–sulfur cluster assembly in the amitochondriate eukaryotes *Trichomonas vaginalis* and *Giardia intestinalis*, as indicated by the phylogeny of IscS. *Mol Biol Evol* **18**, 1919–1928.

Takahashi, Y. & Nakamura, M. (1999). Functional assignment of the *ORF2-iscS-iscU-iscA-hscB-hscA-fdx-ORF3* gene cluster in the assembly of Fe–S clusters in *Escherichia coli*. *J Biochem* **126**, 917–926.

Tangeras, A. (1985). Mitochondrial iron not bound in heme and iron-sulfur centers and its availability for heme-synthesis *in vitro*. *Biochim Biophys Acta* **843**, 199–207.

Thompson, J. D., Gibson, T. J., Plewniak, F., Jeanmougin, F. & Higgins, D. G. (2000). The CLUSTAL X windows interface: flexible strategies for multiple sequence alignment aided by quality analysis tools. *Nucleic Acids Res* **25**, 4876–4882.

Vaňáčová, S., Rasoloson, D., Razga, J., Hrdý, I., Kulda, J. & Tachezy, J. (2001). Iron-induced changes in pyruvate metabolism of *Tritrichomonas foetus* and involvement of iron in expression of hydrogenosomal proteins. *Microbiology* **147**, 53–62.

Vyoral, D. & Petrák, J. (1998a). Detection and quantitation of Fe-59-labeled proteins using storage phosphorimaging. *Anal Biochem* **260**, 103–106.

Vyoral, D. & Petrák, J. (1998b). Iron transport in K562 cells: a kinetic study using native gel electrophoresis and Fe-59 autoradiography. *Biochim Biophys Acta* **1403**, 179–188.

Vyoral, D., Hradílek, A. & Neuwirt, J. (1992). Transferrin and iron distribution in subcellular fractions of K562 cells in the early stages of transferrin endocytosis. *Biochim Biophys Acta* **1137**, 148–154.

Vyoral, D., Petrák, J. & Hradílek, A. (1998). Separation of cellular iron containing compounds by electrophoresis. *Biol Trace Elem Res* **61**, 263–275.

Weaver, J. & Pollack, S. (1989). Low-M_r iron isolated from guinea pig reticulocytes as AMP-Fe and ATP-Fe complexes. *Biochem J* **261**, 787–792.

Weinbach, E. C., Takeuchi, T., Claggett, C. E., Inohue, F., Kon, H. & Diamond, S. D. (1980). Role of iron–sulfur proteins in the electron transport system of *Entamoeba histolytica*. *Arch Investig Med* **11**, 75–81.

Zheng, L., White, R. H., Cash, V. L. & Dean, D. R. (1994). Mechanism for the desulfurization of L-cysteine catalyzed by the *nifS* gene product. *Biochemistry* **19**, 4714–4720.